

# Optical Effects of Ink Spread and Penetration on Halftones Printed by Thermal Ink Jet

*J. S. Arney\* and Michael L. Alber\**

*Rochester Institute of Technology, Rochester, New York 14623*

## Abstract

A probability-based model of halftone imaging, which was developed in previous work to describe the Yule–Nielsen effect, is shown in the current work to be easily modified to account for additional physical and optical effects in halftone imaging. In particular, the effects of ink spread and ink penetration on the optics of halftone imaging with an ink-jet printer is modeled. The modified probability model was found to fit the experimental data quite well. However, the model appears to overcompensate for the scattering associated with ink penetration into paper.

## Introduction

Recent work in this laboratory has been directed at the development of a probability model of the Yule–Nielsen effect to relate fundamental optical properties of papers and inks to tone reproduction in halftone printing. However, practical halftone models also need to account for physical effects such as the lateral spread of ink on the paper, called physical dot gain, and the penetration of ink into the paper. The most fundamental description of the Yule–Nielsen effect involves modeling the optical point spread function, PSF, of light in the paper and convolving the PSF with a geometric description of the halftone dots. Although such models have been shown to be quite accurate in describing the Yule–Nielsen effect, they are computationally quite intensive. Moreover, they are difficult to combine with models of physical dot spread and especially of physical penetration of ink into the paper. But the probability-based model is much less computationally intensive, can be written in a closed analytical form, and is only slightly less rigorous than the convolution approach. Moreover, the probability approach will also be shown to be easily modified to account for ink spread and penetration.

## The Probability Model

The probability model has been described elsewhere,<sup>1,2</sup> and here we present only the recipe for its application. The model begins with an empirical description of the mean probability  $P_p$  that a photon of light that enters the paper between halftone dots will emerge under a dot.

$$P_p = w[1 - (1 - F)^B], \quad (1)$$

where  $F$  is the dot area fraction and  $w$  is the magnitude of the Yule–Nielsen effect and is related quantitatively to the optical point spread function of the paper.<sup>1,2</sup> Both

$F$  and  $w$  can have values from 0 to 1. The  $B$  factor is a constant characteristic of the chosen halftone pattern and the geometric characteristics of the printer. For the printer used in the current work, an HP 1600C thermal ink-jet, a  $B$  factor of 2.0 was found to provide the best correlation between the model and the experimental measurements described below.

A second function needed to model tone reproduction is the probability  $P_i$  that a photon that enters the paper under a halftone dot (having first passed through the dot) then reemerges from the paper under a dot. The two probabilities have been shown to relate as follows.<sup>1</sup>

$$P_i = 1 - P_p \left( \frac{1 - F}{F} \right). \quad (2)$$

We assume initially an ink that is transparent, with no significant scattering. Then, as shown previously, the reflectance of the paper between the dots and of the dots is given by Eqs. 3 and 4, with  $R_g$  the reflectance of the paper on which the halftone pattern is printed.

$$R_p = R_g[1 - P_p(1 - T_i)], \quad (3)$$

$$R_i = R_g T_i[1 - P_i(1 - T_i)]. \quad (4)$$

Note that the reflectance of the ink and of the paper between the dots are not constant but depend on the dot area fraction  $F$  through Eqs. 1 and 2.

With the reflectance of the ink dots and the paper between the dots, the overall reflectance of the halftone image is calculated with the Murray–Davies equation.

$$R(F) = FR_i + (1 - F)R_p. \quad (5)$$

The Yule–Nielsen “ $n$ ” factor is not used in Eq. 5 because the Yule–Nielsen effect is described by the scattering probability  $P_p$ . Thus, to model tone reproduction  $R$  versus  $F$ , one needs (1) the transmittance of the ink  $T_i$ , (2) the reflectance of the paper  $R_g$ , (3) the scattering power of the paper  $w$ , and (4) the geometry factor  $B$ . The value of  $T_i$  can be determined with the Beer–Lambert equation using the coverage of the ink within the dot  $c$  in  $\text{g}/\text{m}^2$  and the extinction coefficient  $\epsilon$  in  $\text{m}^2/\text{g}$ .

$$T_i = 10^{-\epsilon c}. \quad (6)$$

The pigment-based ink was delivered by the printer at  $c = 7.31 \text{ g}/\text{m}^2$ . This was determined by weighing the ink cartridge before and after commanding the printer to print a known number of ink drops at a selected area coverage of 0.50.

As a test of the model, a dispersed-dot halftone at 300 dpi addressability was printed using an HP 1600C

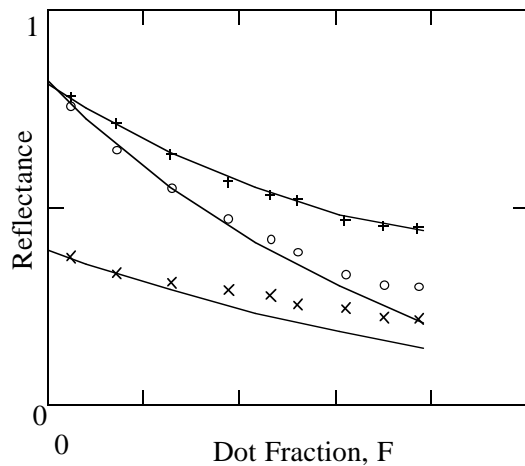


Figure 1. Reflectance versus dot area fraction for the paper between the dot (+), the mean image (o), and the ink (x) for the pigmented magenta ink printed at 300 dpi with a disperse halftone pattern on a commercial gloss paper. The lines are drawn from the model with  $\epsilon = 0.060 \text{ m}^2/\text{g}$  and  $w = 0.75$  with no physical dot gain and no penetration.

thermal ink-jet. Figure 1 shows the measured reflectance of the halftone image  $R$ , the ink dots  $R_p$ , and the paper between the dots  $R_p$  versus the dot area fraction  $F$  measured by microdensitometry as described previously.<sup>1,2</sup> The reflectance values are integral values characteristic of the instrument spectral sensitivity. The solid lines in Fig. 1 are the model calculated as follows: The values of  $R_g$  and  $c$  were measured independently. The values of  $e$  and  $w$  were used as independent variables to provide the best fit between the model and the data. For selected  $e$  and  $w$ , Eq. 6 was applied, then Eqs. 2 through 5. The values of  $e$  and  $w$  were adjusted to provide a minimum rms deviation between the model and experimental values of  $R_p$ . Figure 1 shows that the model describes the paper reflectance  $R_p$ , quite well, but the measured values of  $R_i$  are significantly higher than expected from the model. Clearly, modification of the model to account for nonideal behavior of the thermal ink-jet system is needed.

### Dot Spread and Overlap

A deficiency of the above model is the way in which  $T_i$  is estimated with Eq. 6. The value of  $c = 7.31 \text{ g/m}^2$  was estimated from an accurate measure of ink mass, but the area coverage was estimated as the value commanded by the printer. However, inks can spread out and/or overlap, and this makes the actual ink coverage differ from the commanded ink coverage. This, in turn, changes the transmittance of the ink layer on the paper. To improve the estimate of  $T_i$  in the model, the ideal value of  $c_0 = 7.31 \text{ g/m}^2$  was modified to estimate the actual ink coverage  $c$ . This was done by measuring the actual area coverage  $F$  determined by microdensitometry and comparing it with the value  $F_0$  sent to the printer. The correct value of  $c$  was calculated from Eq. 7.

$$c = c_0 \frac{F}{F_0} \quad c = c_0 \frac{F_0}{F} \quad (7)$$

Due to typographic error, this equation is now displayed properly; (Original print in gray)

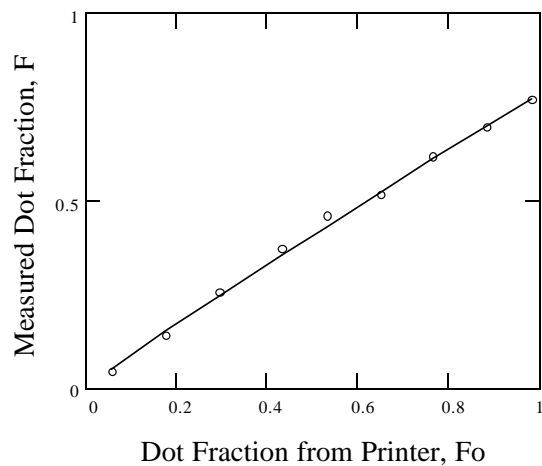


Figure 2. Measured ink area fraction  $F$ , versus the nominal gray fraction  $F_0$  commanded by the printer. The  $F_{\max}$  is the ink area fraction at a nominal gray fraction of  $F_0 = 1.00$ .

To use Eq. 7 in the model, a relationship between  $F$  and  $F_0$  is needed. However, this is a characteristics of a given printer, and rather than model it a priori the effect was characterized experimentally by measuring the printed ink area fraction  $F$  as a function of the value commanded by the printer  $F_0$ . Values of  $F$  were measured by histogram segmentation of images captured by the microdensitometer, as described previously.<sup>1,2</sup> Figure 2 is an example, and the data were fit empirically to Eq. 8 with  $F_{\max} = 0.79$  and  $m = 1.05$ .

$$F = F_{\max} F_0^m \quad (8)$$

The model was then run by ranging  $F$  from 0 to  $F_{\max}$ . At each  $F$  the ratio  $F/F_0$  was calculated using Eq. 8. Equation 7 was then applied to determine  $c$ , which was used in Eqs. 6 and 2 through 5. The values of  $R_g$ ,  $m$ ,  $F_{\max}$ , and  $c_0$  were measured independently, and the values of  $e$  and  $w$  were adjusted to provide a minimum rms deviation between the model and experimental values of  $R_p$ , as shown in Fig. 3. Again fit to  $R_p$  is good, but  $R_i$  is still modeled with a reflectance that is lower than observed experimentally. Indeed, the fit appears worse than in Fig. 1 suggesting that ink spread and overlap, while clearly present in Fig. 2, is not the major perturbation in tone reproduction characteristics of the system. It was anticipated that ink penetration into the paper may have a significant effect.

### Ink Penetration into the Paper

The effect of ink penetration into the substrate could be quite complex. In a a priori model in which the paper PSF is convolved with the halftone pattern, vertical penetration of the dot would require a 3-D convolution and a detailed knowledge of the 3-D geometry of the ink. Such halftone modeling has been described but is quite complex.<sup>3-5</sup> For the current probability model, ink penetration was approximated in a much simpler way. The major optical effect of ink penetration was assumed to be in the increased scattering of light in the ink by the paper. To model the effect we assume the ink behaves as

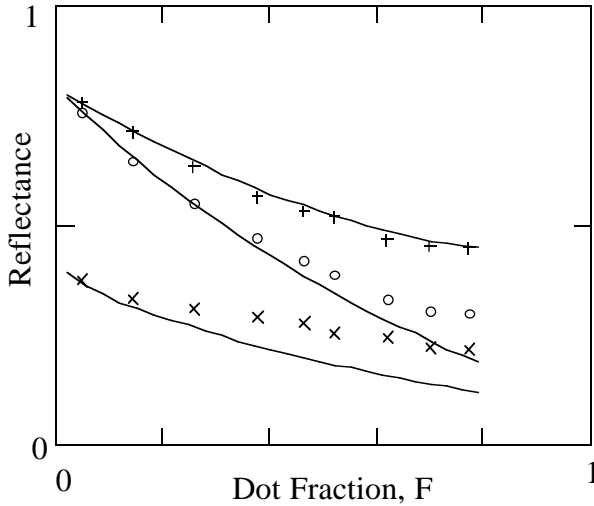


Figure 3. Reflectance versus dot area fraction for the paper between the dot (+), the mean image (o), and the ink (x) for the pigmented magenta ink printed at 300 dpi with a disperse halftone pattern on a commercial gloss paper. The lines are drawn from the model with  $\epsilon = 0.052 \text{ m}^2/\text{g}$ ,  $w = 0.70$ , and  $F_{\max} = 0.79$ .

if it does not actually penetrate the sheet but only increases in scattering coefficient  $S$ . In other words, the model is identical to the case of a nonpenetrating ink with a significant scattering coefficient. Thus an increase in  $S$  is used as an index of the degree of ink penetration into the paper substrate. This scattering effect was added to the probability model as follows:

First, the ink scattering coefficient causes some light to reflect from the ink dot without penetrating through the dot. The Kubelka–Munk model gives this reflectance contribution as follows:<sup>6</sup>

$$R_{iK} = \frac{1}{a + b \cdot \text{Coth}(bSx)}, \quad (9)$$

where  $a = (Sx + Kx)/Sx$  and  $b = (a^2 - 1)^{1/2}$ .

The value of the product  $Kx$  is linearly related to the product  $\epsilon c$ ,

$$Kx = 2.303 \epsilon c, \quad (10)$$

and the product  $Sx$  will be used as an independent variable in the tone reproduction model.

Second, some light penetrates the dot and enters the paper. The transmittance of the dot, according to Kubelka–Munk, is given as follows:

$$T_i = \frac{b}{a \cdot \text{Sinh}(bSx) + b \cdot \text{Cosh}(bSx)} \quad (11)$$

Equation 11 replaces Eq. 6 in the model.

Light that enters the paper between the halftone dots is scattered and may emerge with probability  $P_p$  under the dot. Equation 1 has been used to model this probability for the disperse dot halftone. However, light that encounters a dot with a significant scattering coefficient  $Sx$  may be reflected back into the paper. A detailed description of this effect might include multiple scattered reflections between the substrate and the dot, but a simpler approximation will be used in the current model. One approach might be to assume the effect results in a decrease in the effective value of  $T_i$  of the dot. However, light that fails to transmit through the dot is returned to

the paper where it can scatter and emerge between the dot. This would not be accounted for by simply approximating a decrease in the effective value of  $T_i$ . Alternatively, the effect can be described as a decrease in the probability factor  $P_p$ . In other words, the effect of scattering in the dot can be modeled as a decrease in the probability that light entering the paper between the dots will emerge from the system after passing through the dot. The effect will be approximated by modifying Eq. 1 with the reflectance factor from Eq. 9.

$$P_p = w[1 - (1 - F)^\beta][1 - R_{iK}]. \quad (12)$$

The value of  $P_p$  from Eq. 12 is used to determine  $P_i$  from Eq. 2 and  $R_i$  from a modified form of Eq. 4 in which reflectance from the bulk is added to the Kubelka–Munk reflectance  $R_{KM}$  to produce the overall ink reflectance,

$$R_i = R_g T_i [1 - P_i(1 - T_i)] + R_{iK}. \quad (13)$$

The reflectance of the paper is determined from Eq. 3 as before, and the overall reflectance is determined with Eq. 4. If the Kubelka–Munk reflectance  $R_{KM}$  is zero (no scattering), the model reduces exactly to the model used in Fig. 3. If, however, the scattering  $Sx$  is adjusted as a third independent variable, the result shown in Fig. 4 can be achieved.

## Modifying Ink Spread and Penetration

Achieving the fit of all three nonlinear sets of data in Fig. 4 with only the three independent variables  $\epsilon$ ,  $w$ , and  $Sx$  suggests the model is at least a reasonable approximation of the optical and physical behavior of the ink-jet system. To examine the physical impact of spread and penetration further, the ink and halftone pattern of Fig. 4 was printed on a recycled plain paper. The experimental data and the fit of the model are shown in Fig. 5. Evident from this experiment are the following: First, the model is able to fit the data quite well. Moreover, the fit is achieved with a significantly higher value of  $Sx$  than one would expect for the plain paper system. The ink penetrates farther into the plain paper and thus has a higher effective scattering coefficient. However, the model may overcompensate for this scattering effect in the ink layer and, thus, requires a slightly higher value of  $\epsilon$  to achieve a good fit with the data. Moreover, the value of  $w$  which fits the data is lower for the plain paper than for the gloss-coated paper, which is the reverse of expectation.<sup>7</sup> The value of  $w$  is related to the mean distance light travels between scattering events, and this is expected to be larger in plain papers than in coated papers. Perhaps this effect also has been overcompensated by the simplifying assumptions in modeling ink penetration.

Halftone patterns were also printed for a dye-based ink on both the plain paper and the coated paper. The parameters used to fit the model to the data for all experiments along with the observed values of  $F_{\max}$  are summarized in Table I. In most cases the trends in the parameters are as expected. For example, the measured values of  $F_{\max}$  indicate the amount of lateral spread of ink on the paper and the lateral spread is greater for dye-based ink on the coated paper than on the plain paper. However, the amount of lateral spread is not significantly

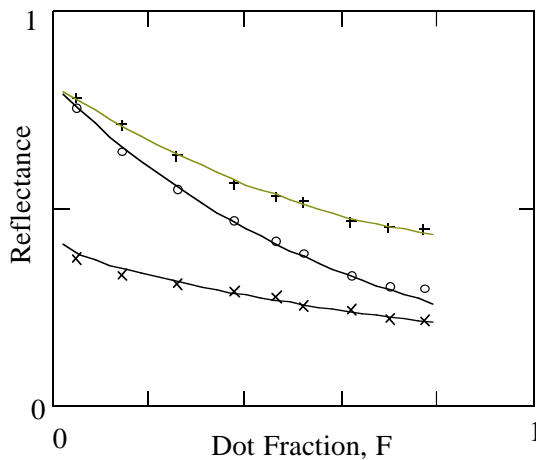


Figure 4. Reflectance versus dot area fraction for the paper between the dot (+), the mean image (o), and the ink (x) for the pigmented magenta ink printed at 300 dpi with a disperse halftone pattern on a commercial gloss paper. The lines are drawn from the model with  $\epsilon = 0.051 \text{ m}^2/\text{g}$  and  $w = 0.73$ , measured dot gain parameters of  $m = 1.05$  and  $F_{\max} = 0.79$ , and ink penetration modeled with  $S_x = 0.5$ .

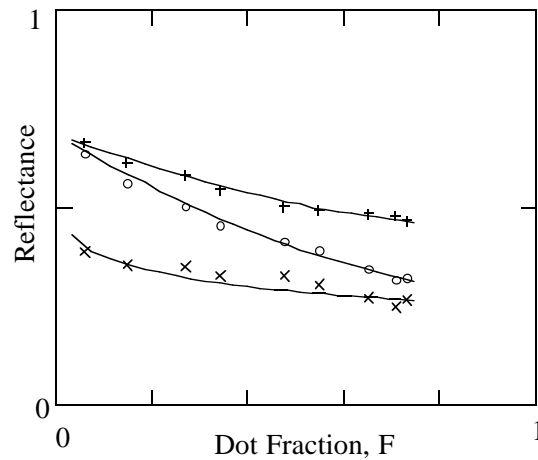


Figure 5. Reflectance versus dot area fraction for the paper between the dot (+), the mean image (o), and the ink (x) for the pigmented magenta ink printed at 300 dpi with a disperse halftone pattern on a recycled plain paper. The lines are drawn from the model with  $\epsilon = 0.06 \text{ m}^2/\text{g}$  and  $w = 0.55$ , measured dot gain parameters of  $m = 1.05$  and  $F_{\max} = 0.79$ , and ink penetration modeled with  $S_x = 1.3$ .

TABLE I. Summary of Modeling Parameters. Parameters Adjusted to Achieve the Minimum rms Deviation Between Model and Data for All Three Sets of Data  $R$ ,  $R_p$ , and  $R_p$  versus  $F$ . Also Shown is the Value of  $F_{\max}$  or the Dot Area Fraction at a Nominal Print Gray Scale of 100%.

Ink base	Paper	$\epsilon \text{ (m}^2/\text{g)}$	$w$	$S_x$	$F_{\max}$
pigment	coated glossy	0.052	0.70	0.50	0.79
dye	coated glossy	0.099	0.75	0.88	0.84
pigment	recycled plain	0.060	0.55	1.3	0.77
dye	recycled plain	0.13	0.55	1.5	1.017

different for the pigmented ink on the two types of paper. But the effective increase in light scattering within the ink dot,  $S_x$ , in going from the coated paper to the plain paper is evident in both the pigment and the dye-based inks. In addition, the value of  $\epsilon$  is higher for the dye-based ink, as is typically observed, but the values should not change when the paper is changed. That it does in both cases suggests the simple model of ink penetration overestimates the optical effect of scattering, requiring a compensating adjustment of  $\epsilon$ .

## Conclusion

The success of the model described in this report indicates the advantage of the probability model for exploring and modeling the mechanism of halftone imaging. Because the probability model can be written in closed analytical form, it is easily modified to account for additional mechanistic effects such as ink spread. Such modifications are much more difficult to do with an a priori model involving the convolution of ink with the paper point spread function. The probability model does, nevertheless, maintain a reasonable connection with the fundamental parameters of the point spread function through the empirical  $w$  parameter<sup>1,2</sup> and through fundamental theory described by Rodgers.<sup>8</sup> Caution should be used, however, in applying the simplifying assumptions

for ink penetration, because the model appears to overcompensate the optics of the penetration effect and to decrease the reliability of the  $w$  parameter as an index of the paper point spread function.

## Acknowledgments

Support for this project was provided by DuPont Corporation and is gratefully acknowledged. Special thanks to Paul Oertel for many challenging discussions and helpful suggestions.

## References

1. J. S. Arney, A probability description of the Yule–Nielsen effect, *J. Imaging Sci. Technol.* **41**(6), 633–636 (1997); *see pg. 451, this publication.*
2. J. S. Arney and M. Katsube, A probability description of the Yule–Nielsen Effect II: The impact of halftone geometry, *J. Imaging Sci. Technol.* **41**(6), 637 (1998); *see pg. 456, this publication.*
3. F. Ruckdeschel and O. G. Hauser, *Appl. Opt.* **17**, 3376 (1978).
4. S. Gustavson, Color gamut of halftone reproduction, *J. Imaging Sci. Technol.* **41**, 283 (1997); *see pg. 443, this publication.*
5. S. Gustavson, Dot gain in color halftones, Ph.D. Dissertation, Kinkoping University Department of Electrical Engineering, Linkoping, Sweden, Fall 1997.
6. G. Wyszecki and W. S. Stiles, *Color Science*, 2nd. ed., John Wiley & Sons, NY, 1982, p. 785.
7. J. S. Arney, C. D. Arney, and M. Katsube, An MTF analysis of paper, *J. Imaging Sci. Technol.* **40**, 19 (1996).
8. G. L. Rogers, Optical dot gain in halftone print, *J. Imaging Sci. Technol.* **41**(6) 643–656 (1997); *see pg. 462, this publication;* Optical dot gain: Lateral scattering probabilities, *J. Imaging Sci. Technol.* **42**(4), 341 (1998); *see pg. 495, this publication.*

\* Previously published in the *Journal of Imaging Science and Technology* **42**(4), pp. 331–334, 1997.